Monthly Notices of the ROYAL ASTRONOMICAL SOCIETY

MNRAS **500,** 3920–3925 (2021) doi:10.1093/mnras/staa3422
Advance Access publication 2020 November 5

Search for giant planets around seven white dwarfs in the Hyades cluster with the *Hubble Space Telescope*

Wolfgang Brandner [1]★ Hans Zinnecker[2,3] and Taisiya Kopytova[1,4,5]

[1]*Max-Planck-Institut für Astronomie, Königstuhl 17, 69117 Heidelberg, Germany*
[2]*Deutsches SOFIA Institut, Unversität Stuttgart, 70569 Stuttgart, Germany*
[3]*Universidad Autonoma de Chile, Avda Pedro de Valdivia 425, Santiago, Chile*
[4]*Division of Medical Image Computing, German Cancer Research Center (DKFZ), 69120 Heidelberg, Germany*
[5]*Ural Federal University, Yekaterinburg 620002, Russia*

Accepted 2020 October 23. Received 2020 October 1; in original form 2020 July 31

ABSTRACT

Only a small number of exoplanets have been identified in stellar cluster environments. We initiated a high angular resolution direct imaging search using the *Hubble Space Telescope* (*HST*) and its Near-Infrared Camera and Multi-Object Spectrometer (NICMOS) instrument for self-luminous giant planets in orbit around seven white dwarfs in the 625 Myr old nearby (≈45 pc) Hyades cluster. The observations were obtained with Near-Infrared Camera 1 (NIC1) in the F110W and F160W filters, and encompass two *HST* roll angles to facilitate angular differential imaging. The difference images were searched for companion candidates, and radially averaged contrast curves were computed. Though we achieve the lowest mass detection limits yet for angular separations ≥0.5 arcsec, no planetary mass companion to any of the seven white dwarfs, whose initial main-sequence masses were >2.8 $M_\odot$, was found. Comparison with evolutionary models yields detection limits of ≈5–7 Jupiter masses ($M_{\rm Jup}$) according to one model, and between 9 and ≈12 $M_{\rm Jup}$ according to another model, at physical separations corresponding to initial semimajor axis of ≥5–8 au (i.e. before the mass-loss events associated with the red and asymptotic giant branch phase of the host star). The study provides further evidence that initially dense cluster environments, which included O- and B-type stars, might not be highly conducive to the formation of massive circumstellar discs, and their transformation into giant planets (with $m \geq 6\ M_{\rm Jup}$ and a ≥6 au). This is in agreement with radial velocity surveys for exoplanets around G- and K-type giants, which did not find any planets around stars more massive than ≈3 $M_\odot$.

Key words: planets and satellites: detection – planets and satellites: dynamical evolution and stability – planets and satellites: formation – planets and satellites: gaseous planets – white dwarfs – open clusters and associations: individual: Hyades.

1 INTRODUCTION

Although several 1000 exoplanets and exoplanet candidates have been identified by now (Perryman 2018; Shabram et al. 2020), less than 1 per cent of these reside in stellar clusters (Kovács et al. 2014). Both radial velocity (RV) surveys (e.g. Paulson et al. 2004; Guenther et al. 2005) and surveys for transiting planets (Gilliland et al. 2000; van Saders & Gaudi 2011; Mann et al. 2016) in populous open and globular cluster confirm the low frequency of close-in planets around cluster members. The RV discovery of a giant exoplanet with ≈7.5 $M_{\rm Jup}$ in a ≈2 au orbit around the 2.7 $M_\odot$ K0 giant ϵ Tau, which is a kinematic member of the Hyades open cluster, led to the suggestion that giant planets around intermediate-mass stars do exist (Sato et al. 2007).

Direct imaging studies for exoplanets need to overcome both the brightness contrast between a star and its exoplanet, and achieve fine angular resolution in order to separate the exoplanet signal from its host star. Similar to brown dwarfs, planets cool with age and are therefore most easily detectable at young ages while they are still self-luminous in the infrared. Indeed direct imaging searches for exoplanets have been most successful around young stars (Chauvin et al. 2005, 2017; Marois et al. 2008; Lagrange et al. 2009; Macintosh et al. 2015; Keppler et al. 2018).

With the aim to search for giant planets in an open cluster environment, we selected white dwarfs in the Hyades. The Hyades, at an age of 625 ± 50 Myr and at an average distance of 45 pc (e.g. Perryman et al. 1998; Kopytova et al. 2016), constitutes the most nearby open cluster. In addition to 724 stellar systems classified by their proper motion as kinematic member candidates (Röser et al. 2011), seven single white dwarfs (see Table 1) and three white dwarfs, which are companions to stars, have been established as Hyades cluster members (Zuckerman & Becklin 1987; von Hippel 1998). Prior to *Gaia* Data Release 2 (DR2) at least six additional white dwarfs were considered likely members of the Hyades cluster (Schilbach & Röser 2012; Tremblay et al. 2012; Zuckerman et al. 2013). Salaris & Bedin (2018) confirm two of these (WD 0348+339 and WD 0400+148) as high probability members. Born as Herbig Ae stars with initial masses in the range 2.8–3.6 $M_\odot$ (Kalirai, Marigo

★ E-mail: brandner@mpia.de

Table 1. Basic astrophysical parameters of the Hyades single white dwarfs and date of *HST*/NICMOS observations.

Name	Alt. name	J (mag)	H (mag)	Distance (pc)	$M_{\rm init}$ ($M_\odot$)	$M_{\rm final}$ ($M_\odot$)	Obs. date
WD 0352+096	HZ 4	14.83 ± 0.04	14.87 ± 0.06	35.0	3.59	0.80	2003-11-04
WD 0406+169	LB 227	15.70 ± 0.07	15.47 ± 0.12	50.2	3.49	0.85	2004-02-07
WD 0421+162	VR 7, LP 415−46	14.75 ± 0.04	14.82 ± 0.06	45.0	2.90	0.70	2004-02-15
WD 0425+168	VR 16, LP 415−415	14.63 ± 0.03	14.65 ± 0.05	47.9	2.79	0.71	2003-11-05
WD 0431+126	HZ 7	14.77 ± 0.03	14.80 ± 0.06	47.3	2.84	0.69	2003-11-06
WD 0437+138	LP 475−242	15.32 ± 0.05	15.51 ± 0.12	46.0	3.41	0.74	2003-11-07
WD 0438+108	HZ 14	14.50 ± 0.04	14.62 ± 0.05	49.4	2.78	0.73	2003-11-09

Note. Apparent magnitudes are from 2MASS; distances are based on *Gaia* DR2 parallaxes (Gaia Collaboration et al. 2016, 2018; Bailer-Jones et al. 2018), which within the uncertainties are in very good agreement with the distances previously reported by Schilbach & Röser (2012); initial and final mass estimates are from Kalirai et al. (2014).

& Tremblay 2014), the circumstellar discs of the white dwarf progenitors could have been the birthplaces of giant planets.

White dwarfs offer two advantages for direct imaging surveys for exoplanets (Zinnecker & Friedrich 2001; Burleigh, Clarke & Hodgkin 2002; Gould & Kilic 2008). First, planets on circular or moderately eccentric orbits with semimajor axis of several astronomical unit (au) would survive the post-main-sequence mass loss of the parent star, and would migrate outward adiabatically by a factor equal to the ratio of initial to final stellar mass due to conservation of orbital angular momentum (e.g. Villaver & Livio 2009; Nordhaus & Spiegel 2013). Secondly, because of their small surface area, white dwarfs are considerably less luminous than their early A- or late B-type main-sequence progenitors, thus alleviating the contrast requirements. The reduced contrast requirements facilitated the first direct imaging detection of a brown dwarf as a companion to the white dwarf GD 165 (Becklin & Zuckerman 1988).

An additional motivation is semi-analytic circumstellar disc models by Kennedy & Kenyon (2008), which predict a linear increase in the occurrence rate of giant planets with stellar mass in the range 0.4–3 $M_\odot$. Direct imaging detections of giant exoplanets orbiting the mid A-type stars HR 8799 (Marois et al. 2008, 2010) and β Pic (Lagrange et al. 2010) might be supportive for these models. With the exception of WD 0806−661 B (Luhman, Burgasser & Bochanski 2011), direct detection spectroscopic and imaging searches for planetary mass companions to white dwarfs were unsuccessful thus far (e.g. Chu et al. 2001; Hogan, Burleigh & Clarke 2011; Xu et al. 2015). Their proximity with distances between 35 and 50 pc (Bailer-Jones et al. 2018), relatively young age, and main-sequence progenitor masses of ≈3 $M_\odot$ make the Hyades cluster white dwarfs promising targets to search for substellar companions at orbital separations of several tens of au.

2 OBSERVATIONS AND DATA REDUCTION

The data were obtained with *Hubble Space Telescope* (*HST*)/Near-Infrared Camera and Multi-Object Spectrometer (NICMOS) (GO 9737, PI: H. Zinnecker). Table 1 lists the target sample, basic astrophysical parameters, and the date of the *HST* observations. The data were obtained with Near-Infrared Camera 1 (NIC1) in MULTIACCUM mode (NSAMP=18, STEP32), applying a two-point dither pattern with the science targets centred in the top-right or bottom-right quadrant, respectively, and two telescope roll angles differing by 20°. The latter facilitates the application of the angular differential imaging technique for high-contrast subtraction of static point spread function (PSF) structures (Müller & Weigelt 1987; Lafrenière et al. 2007). Total integration times in F110W and F160W amount to 1280 and 2560 s, respectively, for each of the white dwarfs.

The raw data were pre-reduced with CALNICA, version 4.4.1. Compared to earlier reductions of this data set (Zinnecker et al. 2006; Friedrich et al. 2007; Zinnecker & Kitsionas 2008), the re-reduction included a temperature-dependent dark correction. This resulted in a better background subtraction, and overall improved contrast ratios in particular at larger angular separations.

The subsequent data reduction steps consisted of the following.

(i) Pairwise subtraction of dithered positions to remove residual background, and visual inspection for wide companion candidates.
(ii) Alignment and subtraction of individual 64 × 64 pixels subfields centred on the white dwarf for two roll angles to facilitate angular differential imaging (removal of static PSF pattern).
(iii) Combination and visual inspection of difference frames. Real sources should show up as a positive and negative PSF at the same separation from the white dwarf, and with instrumental position angles differing by 20°[1] (see Fig. 1).
(iv) Computation of the residual noise pattern in annuli centred on the white dwarf. The radial 3σ brightest pixel detection limits for each white dwarf are shown in Fig. 2.

The contrast curves asymptotically approach the background limit for separations ≥0.6 arcsec. At a separation of 0.5 arcsec the achievable contrast is still subject to PSF residuals. With the exception of WD 0406+169, longer exposure times would not have significantly improved the contrast. At angular distances ≥0.5 arcsec from the white dwarf, the detection limit for the full sample is in the range $m_{\rm F110W}$ = 22.9–23.5 mag and $m_{\rm F160W}$ = 22.2–22.9 mag. The actual brightness differences (3σ detection limits) at 0.5 arcsec are $\Delta m_{\rm F110W}$ = 7.8–8.6 mag and $\Delta m_{\rm F160W}$ = 6.7–7.8 mag (see Table 2).

Orbits of confirmed exoplanets with semimajor axis between 4 and 20 au have a mean eccentricity of ≈0.35.[2] Assuming similar orbital parameters for our sample, we applied a correction factor of 1/0.83 for the conversion from projected separations to semimajor axis (see e.g. Leinert et al. 1993 for a derivation).

3 FLUX AND MASS DETECTION LIMITS ON EXOPLANETS

Starting from the 3σ $\Delta m_{\rm F110W}$ and $\Delta m_{\rm F160W}$ contrast detection limits and the apparent Two Micron All-Sky Survey (2MASS) J

[1]For WD 0421+162 the observations of the first *HST* orbit in F160W are all obtained at the same roll angle. We averaged all observations from this and the second orbit with the same roll angle, and subtracted the one dithered data set obtained in the second *HST* orbit at the 20° offset roll angle.
[2]http://exoplanet.eu

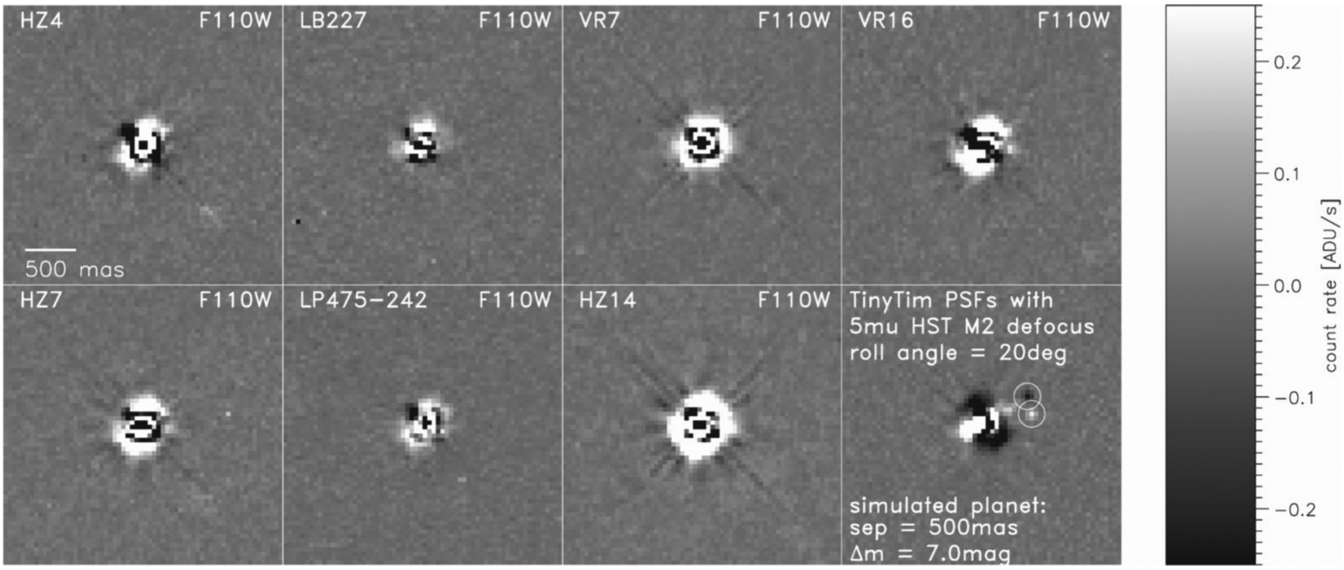

Figure 1. Roll subtracted images of the *HST* NIC1 observations in F110W of the seven white dwarfs (left to right, top to bottom) and simulated observations based on TINY TIM PSF simulations (Krist, Hook & Stoehr 2011) with an exoplanet at a separation of 500 mas, and 7.0 mag fainter than the white dwarf (lower right).

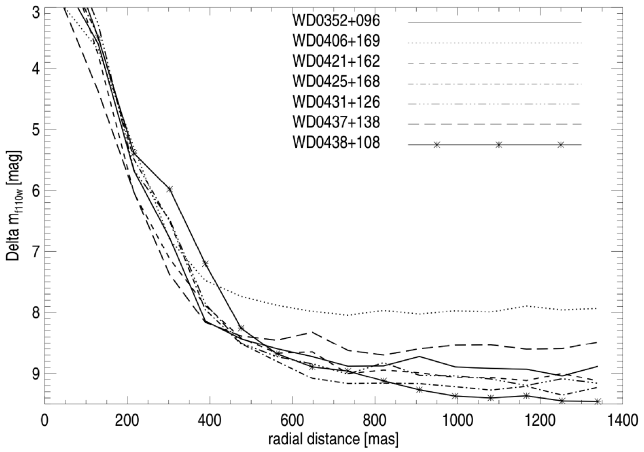

Figure 2. Brightness contrast (3σ) in F110W versus angular separation for the seven white dwarfs, reaching $\Delta m_{\rm F110W} > 8$ mag beyond 500 mas.

and *H* magnitudes of the white dwarfs, we calculated the detection limits for companions in terms of apparent magnitudes. The apparent magnitudes were converted to absolute magnitudes using *Gaia* DR2 parallax measurements for comparison with theoretical evolutionary models for substellar objects.

We selected evolutionary models for substellar objects with solar metallicity by Baraffe et al. (2003) and Spiegel & Burrows (2012). In the latter case, we consider 'hybrid' (i.e. a linear combination of cloud and cloud-free) atmospheric models with either high-entropy (hothycl) or low-entropy (coldhycl) initial conditions. For the transformation of brightness limits into mass limits the canonical age of the Hyades of 625 Myr was assumed. It is noted that according to the models even at this relatively advanced age, the most massive exoplanets still retain a 'memory' of the starting conditions, i.e. the derived mass estimates assuming a cold start are typically 2 $M_{\rm Jup}$ higher than for a hot start. The presence or absence of atmospheric condensation layers ('DUSTY' or 'COND' following the notation by Allard et al. 2001), and variations of the metallicity result in uncertainties of the same order. As the models by Spiegel & Burrows (2012) are limited to masses $\leq$10 $M_{\rm Jup}$, in some cases we used an extrapolation to estimate mass limits.

Also shown in Table 2 are the mass limits derived from *Spitzer* Infrared Array Camera (IRAC) observations in the 4.5 μm band according to Farihi, Becklin & Zuckerman (2008), which are based on the models by Baraffe et al. (2003), and assuming a uniform distance of 46 pc towards all of the white dwarfs.

In all cases, observations in F110W provided lower mass limits, and thus tighter constraints than the observations in F160W. Overall mass limits are in the range of 4.6–6.7 $M_{\rm Jup}$ assuming the models by Baraffe et al. (2003). Hybrid clouds and hot start models (Spiegel & Burrows 2012) place detection limits in the range 8–10 $M_{\rm Jup}$. Thus irrespective of the model set we choose, we should be able to detect brown dwarf companions with masses $\geq$12 $M_{\rm Jup}$ at current angular separations $\geq$0.5 arcsec to any of the seven white dwarfs in the sample. In case the models by Baraffe et al. (2003) are applicable, the average detection limit corresponds to exoplanets with masses in excess of $\approx$5.6 $M_{\rm Jup}$, which represents an improved detection limit for resolved exoplanet companions compared to the (indirect) average limit of $\approx$9.4 $M_{\rm Jup}$ from *Spitzer*/IRAC (Farihi et al. 2008).

4 DISCUSSION

Present-day mass estimates for Hyades white dwarfs have been derived from analysis of spectroscopic data using atmospheric models (Bergeron et al. 2011; Gianninas, Bergeron & Ruiz 2011). We note that gravitational redshift measurements for a subset of the Hyades white dwarfs yield 5–10 per cent lower mass estimates (Pasquini et al. 2019). For the following discussion, we consider this small systematic discrepancy in mass estimates of minor importance.

The Hyades white dwarf progenitors lost about 75 per cent of their initial mass (Kalirai et al. 2014). Because of conservation of orbital angular momentum during the red giant (RG)/asymptotic giant branch (AGB) phase any surviving stellar or substellar companion must have migrated outward adiabatically, enlarging the semimajor axis of its orbit by a factor of 3.8–4.6 (ratio of initial stellar to

Table 2. Detection limits at an angular separation ≥0.5 arcsec in F110W and F160W: brightness difference, 3σ apparent and absolute magnitude limit, corresponding upper mass limit for substellar companions according to evolutionary and atmospheric models, and current and initial projected physical separation corresponding to 0.5 arcsec based on mass-loss estimates for the white dwarf progenitors and assuming a typical orbital eccentricity of 0.35. Mass limits at 4.5 μm are from Farihi et al. (2008) and are based on Baraffe models.

Name: WD...	0352+096	0406+169	0421+162	0425+168	0431+126	0437+138	0438+108
$\Delta m_{\rm F110W}$ (mag)	8.48	7.79	8.60	8.59	8.62	8.35	8.39
$m_{\rm limF110W}$ (mag)	23.31	23.49	23.35	23.22	23.39	23.67	22.89
$M_{\rm limF110W}$ (mag)	20.6	20.0	20.1	19.8	20.0	20.4	19.4
$\rm Mass_{Baraffe}$ ($M_{\rm Jup}$)	4.6	5.7	5.5	6.2	5.7	4.9	6.7
$\rm Mass_{hothycl}$ ($M_{\rm Jup}$)	7.7	8.6	8.5	9.0	8.6	8.0	9.6
$\rm Mass_{coldhycl}$ ($M_{\rm Jup}$)	9.1	10.3[a]	10.1[a]	10.8[a]	10.3[a]	9.5	11.7[a]
$\Delta m_{\rm F160W}$ (mag)	7.74	6.70	7.50	7.80	7.65	7.35	7.63
$m_{\rm limF160W}$ (mag)	22.61	22.18	22.31	22.45	22.46	22.86	22.26
$M_{\rm limF160W}$ (mag)	19.9	18.7	19.0	19.0	19.1	19.5	18.8
$\rm Mass_{Baraffe}$ ($M_{\rm Jup}$)	5.9	8.2	7.2	7.2	7.0	6.5	7.8
$\rm Mass_{hothycl}$ ($M_{\rm Jup}$)	8.3	10.0	9.5	9.5	9.4	8.8	9.8
$\rm Mass_{coldhycl}$ ($M_{\rm Jup}$)	9.8	12.1[a]	11.5[a]	11.5[a]	11.3[a]	10.5[a]	11.9[a]
$\rm Mass_{4.5\ \mu m}$ ($M_{\rm Jup}$)	10	7	10	10	10	8	11
$a_{\rm curr}$ (au)	21	30	27	29	28	28	30
$a_{\rm init}$ (au)	4.7	7.4	6.5	7.3	6.9	6.0	7.8

Note. we selected models for solar metallicity by Baraffe et al. (2003) and Spiegel & Burrows (2012). In the latter case, the mass estimates are based on models assuming hybrid clouds and either a hot (hothycl) or a cold (coldhycl) start.
[a]Indicates that the mass limits are based on extrapolation beyond the mass range covered by the models.

final white dwarf mass, see Table 1). Giant planets with initial semimajor axis of their orbits $\gtrapprox$5 au would have survived the post-main-sequence mass loss of the parent star (e.g. Villaver & Livio 2009; Nordhaus & Spiegel 2013), and could now be found in orbits with semimajor axis $\gtrapprox$20–30 au. The latter corresponds to angular separations ≥0.5 arcsec, which we probe in our *HST*/NICMOS survey. The present survey does not probe for planets initially in closer orbits (<2–3 au), which during the RG/AGB phase might have merged with the star due to dynamical friction and tidal interactions (Mustill et al. 2013; Veras et al. 2014).

The NICMOS observations confirm that all seven white dwarfs are single objects. Based on the detection limits and irrespective of evolutionary model we choose, we can rule out brown dwarf companions with masses ≥12 $M_{\rm Jup}$ to any of the white dwarfs at current projected separations ≥18–25 au.

Fig. 3 visualizes the depth of search of our survey based on the models by Baraffe et al. (2003). We convert radial distances from the contrast curves (Fig. 2) into present-day physical separations, and initial semimajor axis during the main-sequence phase of the host stars based on the white dwarf mass-loss estimates. The detection probabilities were calculated assuming planetary orbits with an eccentricity of 0.35 seen from 8000 uniformly distributed viewing angles and at 126 orbital phases distributed uniformly in time. Compared to a search with *Spitzer*/IRAC using infrared excess of the white dwarfs as an indicator for unresolved very low mass companions (Farihi et al. 2008), our mass limits for resolved giant planets at angular separations ≥500 mas are on average ≈4 $M_{\rm Jup}$ lower. Our survey reaches a 50 per cent depth of search at ≈6 $M_{\rm Jup}$ and for an initial semimajor axis of 6 au. Ground-based adaptive optics assisted direct imaging surveys for giant exoplanets, which focus on young stars in the solar neighbourhood, in general probe an overlapping part of the parameter space. For stars more massive than 1.5 $M_\odot$, the Gemini Planet Imager Exoplanet Survey (GPIES) at Gemini South (Nielsen et al. 2019) reaches a 50 per cent depth of search at ≈6 $M_{\rm Jup}$ for semimajor axis ≥50 au. The SpHere INfrared survey for Exoplanets (SHINE) survey at the Very Large

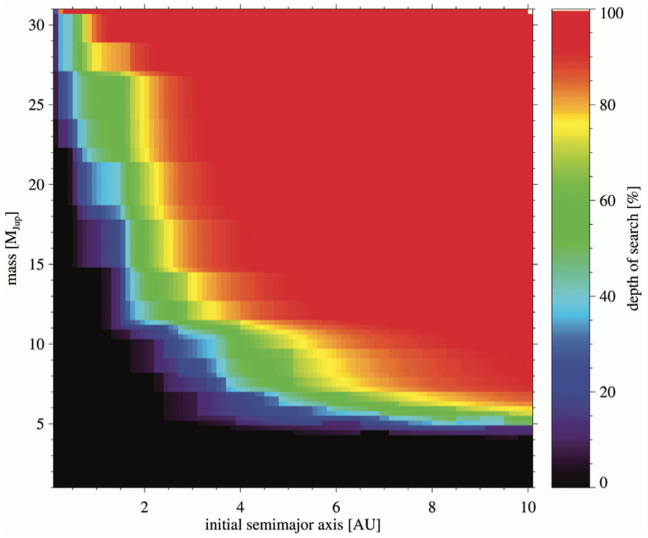

Figure 3. Depth of search, indicating the completeness of the survey of the seven white dwarfs with respect to companion mass and semimajor axis for an assumed typical orbital eccentricity of 0.35. The green colour marks a detection probability of ≈50 per cent, while the red colour corresponds to $\gtrapprox$90 per cent.

Telescope (VLT; Vigan et al. 2020) reports for spectral types M to B, a 50 per cent depth of survey at 6 $M_{\rm Jup}$ for semimajor axis ≥15–20 au.

While our sample of seven single white dwarfs is small, it provides further evidence that initially dense cluster environments, which included O and early B stars, might not be highly conducive for the formation and transformation of massive circumstellar discs around stars with masses ≥2.8 $M_\odot$ into giant planets with semimajor axes ≥6 au and with ≥6 $M_{\rm Jup}$. This is in agreement with the RV survey for exoplanets around 373 G- and K-type giants by Reffert et al. (2015), which did not find any planets around giants with initial main-sequence masses higher than 2.7 $M_\odot$. Other high contrast direct

imaging searches for planetary mass companions to nearby white dwarfs also did not yield any direct detections (Debes, Sigurdsson & Woodgate 2005; Farihi, Zuckerman & Becklin 2005; Debes, Ge & Ftaclas 2006; Xu et al. 2015) apart from GD 165AB.

Indirect evidence for the presence of planets has been derived from abundance anomalies in white dwarf atmospheres and in their accretion discs and from the longevity of debris discs (e.g. Zuckerman et al. 2010, 2013; Farihi, Gänsicke & Koester 2013; Bergfors et al. 2014; Xu et al. 2019). Using optical spectroscopy, Gänsicke et al. (2019) reported strong evidence for a photoevaporating giant planet in close (15 $R_{\odot}$) orbit around a hot white dwarf (WD 1145+017); see also an earlier case suggested by Chu et al. (2001). Recently Vanderburg et al. (2020) announced the detection of a transiting giant planet in a 1.4-d orbit around the relatively old WD 1856+534.

In the Hyades, several Earth- to Neptune-sized exoplanets and exoplanet candidates transiting K- and M-dwarfs were identified with *K2* (Mann et al. 2016; Ciardi et al. 2018; Livingston et al. 2018; Vanderburg et al. 2018). The 2.7 $M_{\odot}$ K-giant ϵ Tau still remains the most massive Hyades member known to host a (giant) exoplanet (Sato et al. 2007).

The divergence of mass estimates between the different evolutionary models and the underlying uncertainty about the starting conditions in the formation of substellar objects highlights the importance of testing and calibrating evolutionary models. This requires both independent mass estimates via astrometric or RV reflex motion of the host star, and studies of the early formation phases of exoplanets. Extremely Large Telescope (ELT) equipped with laser guide star adaptive optics systems could probe the Hyades white dwarfs for giant planets at closer projected separations, and lower mass limits. ELT/Multi-AO Imaging Camera for Deep Observations (MICADO) is expected to achieve a contrast of $\Delta H \approx 14.8$ mag at an angular separation of 500 mas (Perrot et al. 2018), and thus (according to the model by Baraffe et al. 2003) could detect planets with 1–2 $M_{\rm Jup}$ orbiting a white dwarf in the Hyades cluster. In the *K*-band *James Webb Space Telescope* (*JWST*)/Near-Infrared Camera (NIRCam) is predicted to achieve a contrast of $\Delta m_{\rm F210M} \approx 11.5$ mag at 500 mas (Beichman et al. 2010), which yields mass detection limits of the same order as the present *HST*/NICMOS study in F110W (giant planets in the mass and age range under consideration are considerably fainter in the *K* band than in the *J* and *H* bands due to molecular opacities in their atmospheres). The larger collecting area, and improved detector technology of *JWST*/Mid-Infrared Instrument (MIRI) relative to *Spitzer*/IRAC will provide a considerably improved sensitivity for detecting infrared excess from unresolved companions, and might also reach detection limits of 1–2 $M_{\rm Jup}$ for the Hyades white dwarfs.

ACKNOWLEDGEMENTS

We thank S. Reffert, S. Röser, J. van Cleve, and S. Xu for helpful comments on a draft of the paper.

This paper is based on observations made with the NASA/ESA *Hubble Space Telescope* (GO 9737), obtained from the data archive at the Space Telescope Science Institute (STScI). STScI is operated by the Association of Universities for Research in Astronomy, Inc. under NASA contract NAS 5-26555.

This publication makes use of data products from the Two Micron All Sky Survey, which is a joint project of the University of Massachusetts and the Infrared Processing and Analysis Center/California Institute of Technology, funded by the National Aeronautics and Space Administration and the National Science Foundation.

This work has made use of data from the European Space Agency (ESA) mission *Gaia* (https://www.cosmos.esa.int/gaia), processed by the *Gaia* Data Processing and Analysis Consortium (DPAC, https://www.cosmos.esa.int/web/gaia/dpac/consortium). Funding for the DPAC has been provided by national institutions, in particular the institutions participating in the *Gaia* Multilateral Agreement.

DATA AVAILABILITY

The data underlying this paper is available online from the Barbara A. Mikulski Archive for Space Telescopes. The final data products will be shared by the corresponding author on request.

REFERENCES

Allard F., Hauschildt P. H., Alexander D. R., Tamanai A., Schweitzer A., 2001, ApJ, 556, 357
Bailer-Jones C. A. L., Rybizki J., Fouesneau M., Mantelet G., Andrae R., 2018, AJ, 156, 58
Baraffe I., Chabrier G., Barman T. S., Allard F., Hauschildt P. H., 2003, A&A, 402, 701
Becklin E. E., Zuckerman B., 1988, Nature, 336, 656
Beichman C. A. et al., 2010, PASP, 122, 162
Bergeron P. et al., 2011, ApJ, 737, 28
Bergfors C., Farihi J., Dufour P., Rocchetto M., 2014, MNRAS, 444, 2147
Burleigh M. R., Clarke F. J., Hodgkin S. T., 2002, MNRAS, 331, L41
Chauvin G. et al., 2005, A&A, 438, L29
Chauvin G. et al., 2017, A&A, 605, L9
Chu Y.-H., Dunne B. C., Gruendl R. A., Brandner W., 2001, ApJ, 546, L61
Ciardi D. R. et al., 2018, AJ, 155, 10
Debes J. H., Sigurdsson S., Woodgate B. E., 2005, AJ, 130, 1221
Debes J. H., Ge J., Ftaclas C., 2006, AJ, 131, 640
Farihi J., Zuckerman B., Becklin E. E., 2005, Astron. Nachr., 326, 964
Farihi J., Becklin E. E., Zuckerman B., 2008, ApJ, 681, 1470
Farihi J., Gänsicke B. T., Koester D., 2013, MNRAS, 432, 1955
Friedrich S., Zinnecker H., Correia S., Brandner W., Burleigh M., McCaughrean M., 2007, in Napiwotzki R., Burleigh M. R., eds, ASP Conf. Ser. Vol. 372, 15th European Workshop on White Dwarfs. Astron. Soc. Pac., San Francisco, p. 343
Gaia Collaboration et al., 2016, A&A, 595, A1
Gaia Collaboration et al., 2018, A&A, 616, A1
Gänsicke B. T., Schreiber M. R., Toloza O., Fusillo N. P. G., Koester D., Manser C. J., 2019, Nature, 576, 61
Gianninas A., Bergeron P., Ruiz M. T., 2011, ApJ, 743, 138
Gilliland R. L. et al., 2000, ApJ, 545, L47
Gould A., Kilic M., 2008, ApJ, 673, L75
Guenther E. W., Paulson D. B., Cochran W. D., Patience J., Hatzes A. P., Macintosh B., 2005, A&A, 442, 1031
Hogan E., Burleigh M. R., Clarke F. J., 2011, in Schuh S., Drechsel H., Heber U., eds, AIP Conf. Proc. Vol. 1331, Planetary Systems Beyond the Main Sequence: Proceedings of the International Conference. Am. Inst. Phys., New York, p. 271
Kalirai J. S., Marigo P., Tremblay P.-E., 2014, ApJ, 782, 17
Kennedy G. M., Kenyon S. J., 2008, ApJ, 673, 502
Keppler M. et al., 2018, A&A, 617, A44
Kopytova T. G., Brandner W., Tognelli E., Prada Moroni P. G., Da Rio N., Röser S., Schilbach E., 2016, A&A, 585, A7
Kovács G. et al., 2014, MNRAS, 442, 2081
Krist J. E., Hook R. N., Stoehr F., 2011, Proc. SPIE, 8127, 81270J
Lafrenière D., Marois C., Doyon R., Nadeau D., Artigau É., 2007, ApJ, 660, 770
Lagrange A.-M. et al., 2009, A&A, 493, L21
Lagrange A. M. et al., 2010, Science, 329, 57
Leinert C., Zinnecker H., Weitzel N., Christou J., Ridgway S. T., Jameson R., Haas M., Lenzen R., 1993, A&A, 278, 129
Livingston J. H. et al., 2018, AJ, 155, 115

Luhman K. L., Burgasser A. J., Bochanski J. J., 2011, ApJ, 730, L9
Macintosh B. et al., 2015, Science, 350, 64
Mann A. W. et al., 2016, ApJ, 818, 46
Marois C., Macintosh B., Barman T., Zuckerman B., Song I., Patience J., Lafrenière D., Doyon R., 2008, Science, 322, 1348
Marois C., Zuckerman B., Konopacky Q. M., Macintosh B., Barman T., 2010, Nature, 468, 1080
Müller M., Weigelt G., 1987, A&A, 175, 312
Mustill A. J., Villaver E., Veras D., Bonsor A., Wyatt M. C., 2013, EPJ Web Conf., 47, 06008
Nielsen E. L. et al., 2019, AJ, 158, 13
Nordhaus J., Spiegel D. S., 2013, MNRAS, 432, 500
Pasquini L., Pala A. F., Ludwig H. G., Leao I. C., de Medeiros J. R., Weiss A., 2019, A&A, 627, L8
Paulson D. B., Saar S. H., Cochran W. D., Henry G. W., 2004, AJ, 127, 1644
Perrot C., Baudoz P., Boccaletti A., Rousset G., Huby E., Clénet Y., Durand S., Davies R., 2018, preprint (arXiv:1804.01371)
Perryman M., 2018, The Exoplanet Handbook, 2nd edn. Cambridge Univ. Press, Cambridge
Perryman M. A. C. et al., 1998, A&A, 331, 81
Reffert S., Bergmann C., Quirrenbach A., Trifonov T., Künstler A., 2015, A&A, 574, A116
Röser S., Schilbach E., Piskunov A. E., Kharchenko N. V., Scholz R.-D., 2011, A&A, 531, A92
Salaris M., Bedin L. R., 2018, MNRAS, 480, 3170
Sato B. et al., 2007, ApJ, 661, 527
Schilbach E., Röser S., 2012, A&A, 537, A129
Shabram M. I. et al., 2020, AJ, 160, 16
Spiegel D. S., Burrows A., 2012, ApJ, 745, 174
Tremblay P.-E., Schilbach E., Röser S., Jordan S., Ludwig H.-G., Goldman B., 2012, A&A, 547, A99
Vanderburg A. et al., 2018, AJ, 156, 46
Vanderburg A. et al., 2020, Nature, 585, 363
van Saders J. L., Gaudi B. S., 2011, ApJ, 729, 63
Veras D., Evans N. W., Wyatt M. C., Tout C. A., 2014, MNRAS, 437, 1127
Vigan A. et al., 2020, A&A, preprint (arXiv:2007.06573)
Villaver E., Livio M., 2009, ApJ, 705, L81
von Hippel T., 1998, AJ, 115, 1536
Xu S., Ertel S., Wahhaj Z., Milli J., Scicluna P., Bertrang G. H. M., 2015, A&A, 579, L8
Xu S., Dufour P., Klein B., Melis C., Monson N. N., Zuckerman B., Young E. D., Jura M. A., 2019, AJ, 158, 242
Zinnecker H., Friedrich S., 2001, Astron. Ges. Meeting Abstr., 18, #MS 04 04
Zinnecker H., Kitsionas S., 2008, in Fischer D., Rasio F. A., Thorsett S. E., Wolszczan A., eds, ASP Conf. Ser. Vol. 398, Extreme Solar Systems. Astron. Soc. Pac., San Francisco, p. 155
Zinnecker H., Correia S., Brandner W., Friedrich S., McCaughrean M., 2006, in Aime C., Vakili F., eds, Proc. IAU Colloq. #200, Direct Imaging of Exoplanets: Science & Techniques. Cambridge Univ. Press, Cambridge, p. 19
Zuckerman B., Becklin E. E., 1987, ApJ, 319, L99
Zuckerman B., Melis C., Klein B., Koester D., Jura M., 2010, ApJ, 722, 725
Zuckerman B., Xu S., Klein B., Jura M., 2013, ApJ, 770, 140

This paper has been typeset from a TEX/LATEX file prepared by the author.